

Reviews

Cluster models in the quantum-chemical analysis of coordination of nitroxide probes to Lewis acid sites on the surface of Al_2O_3

N. D. Chuvylkin,^{a*} A. M. Tokmachev,^b A. V. Fionov,^b and E. V. Lunina^b

^aN. D. Zelinsky Institute of Organic Chemistry, Russian Academy of Sciences,
47 Leninsky prosp., 117913 Moscow, Russian Federation.

Fax: 007 (095) 135 5328

^bDepartment of Chemistry, M. V. Lomonosov Moscow State University,
Vorob'evy Gory, 119899 Moscow, Russian Federation.

Fax: 007 (095) 939 4575

The results of ESR-spectroscopic and quantum-chemical investigations of the coordination of 2,2,6,6-tetramethylpiperidine *N*-oxyl, 2,2,3,4,5,5-hexamethyl-3-imidazolidine *N*-oxyl, 2,2,4,5,5-pentamethyl-3-imidazoline *N*-oxyl, 2,4,5,5-tetramethyl-2-phenyl-3-imidazoline *N*-oxyl, and 2,4,5,5-tetramethyl-2-octyl-3-imidazoline *N*-oxyl to Lewis acid sites (LAS) on alumina surface are described systematically and analyzed. The cluster models of LAS accepted in radiospectroscopy and based on experimental data on *g*-factors and hyperfine coupling constants with N and Al nuclei in the corresponding donor-acceptor complexes are discussed. Within the framework of the unrestricted Hartree–Fock (UHF) method using the STO-3G, STO-6G, 3-21G, and 6-31G basis sets and also in terms of semiempirical MNDO, AM1, and PM3 procedures, comparative quantum-chemical analysis of the structural, spin, electrostatic, energy, and radiospectroscopic characteristics of the coordination of the model cluster LAS to the simplest representative of nitroxides is performed. Three illustrative types of structures of the resulting surface complex are considered. A semiquantitative interpretation of the whole set of features found experimentally for the coordination of nitroxide probes to the surface LAS on alumina is given.

Key words: quantum-chemical analysis, nonempirical and semiempirical methods, alumina, Lewis acid sites, nitroxide probes, surface donor-acceptor complexes; structural, magnetic resonance, electrostatic, and energy characteristics of coordination.

Introduction

The method of paramagnetic complexes of probe molecules is widely used in the studies of the acidic properties of oxide catalysts and the structures of the proton and Lewis acid sites (LAS) on a surface. Stable nitroxides are used most often as convenient and informative probes. When these species are adsorbed on

oxides possessing proton and Lewis acidity, donor-acceptor surface complexes (SC) are formed; these complexes, like the initial nitroxides themselves, have been studied systematically by ESR spectroscopy.^{1–6}

If the paramagnetic N—O group in the nitroxide participates directly in the formation of the SC, the ESR spectral pattern usually changes. In addition, hyperfine coupling (HFC) both with the ¹⁴N nucleus of the ni-

troxyl group of the radical and with the magnetic nucleus of the cation in the surface LAS is often manifested in the spectra. To date, owing to radiospectroscopic studies of adsorbed radicals, detailed information about the surface of gallium and aluminum oxides and some aluminosilicates has been gained, and conclusions about the structure of LAS and the SC formed by them have been drawn.²⁻⁵ 2,2,6,6-Tetramethylpiperidine *N*-oxyl (tanane) (1), 2,2,3,4,5,5-hexamethyl-3-imidazolidine *N*-oxyl (2), 2,2,4,5,5-pentamethyl-3-imidazoline *N*-oxyl (3), 2,4,5,5-tetramethyl-2-phenyl-3-imidazoline *N*-oxyl (4), and 2,4,5,5-tetramethyl-2-octyl-3-imidazoline *N*-oxyl (5) (Scheme 1) are the probes used most often for this purpose. In this paper, we describe systematically and compare the results of radiospectroscopic and quantum-chemical studies on the coordination of these paramagnetic probes to the surface LAS of alumina.

Models of LAS accepted in radiospectroscopy

The dehydroxylated surface of alumina is characterized by the presence of incompletely coordinated, electron-acceptor Al atoms acting as LAS and by weak Brønsted acidity. Nitroxides form stable paramagnetic complexes with the LAS on the oxide surface. According to ESR spectroscopy, this is accompanied by an increase in the spin density on ¹⁴N and by its appearance on ²⁷Al. As a result of these changes, hyperfine structure from the Al nucleus appears in the ESR spectrum and the constant of HFC with the N nucleus increases.²⁻⁵

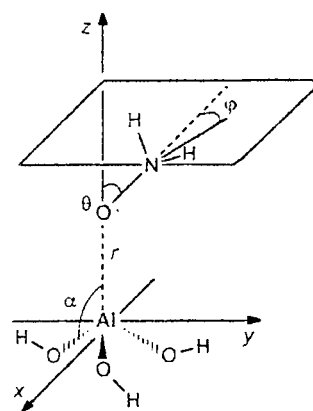
Many aspects concerning the structure and reactivity of the LAS on alumina surface are still unknown and have been the objects of numerous investigations. Some models have been proposed in which the LAS are represented as unsaturated Al³⁺ ions with coordination numbers ranging from 3 to 5. The strongest LAS correspond to a coordination number equal to 3. Therefore, it is generally accepted in radiospectroscopy that the LAS involved in the formation of SC with nitroxides are truncated tetrahedra with a coordination number of 3 resulting from dehydroxylation of the near-surface aluminum-oxygen tetrahedra. The predominant existence of these LAS on the surface of dehydroxylated alumina is also indicated by the fact that the magnetic-resonance parameters (*g*-factors and HFC constants) of the paramagnetic SC formed in this case are virtually identical with those found by ESR spectroscopy for similar complexes of nitroxides with AlCl₃ in nonpolar solvents.²

Radiospectroscopic studies of paramagnetic SC provide only indirect and rather incomplete information on the structures and properties of LAS on the alumina surface. Based on the ESR spectra alone, one cannot determine particular geometric characteristics of these surface LAS. Therefore, an attempt has been undertaken⁷ to increase the information content of the recorded ESR spectra by means of theoretical determination of the magnetic-resonance characteristics of the paramagnetic SC of nitroxides with the hypothetical

LAS as a function of their geometry. This was accomplished using the CINDORU unified cluster procedure,⁸ which had been widely tested⁹ in analogous structure-chemical studies. In these studies, models of paramagnetic surface species had been constructed taking into account the principles¹⁰ of selection and quantum-chemical analysis of the minimum SC.

It should be emphasized that the simplified theoretical simulation⁷ of the experimentally studied interactions of tanane and di-*tert*-butylnitroxyl with the strongest LAS was performed within the framework of the cluster quantum-chemical method of boundary pseudo-ions.¹¹ This means that these LAS were represented as noncharged ionic cluster shareholder, [Al³⁺(O_b^{q-2})₃], consisting of an ordinary Al³⁺ ion and boundary O_b^{q-2} pseudo-ions. The latter belong equally to the AlO₃ cluster fragment itself and to the surrounding Al₂O₃ lattice, the negative charge (-3) of the purely ionic Al³⁺O₃²⁻ cluster being completely neutralized by the identical positive charges *q* = 1 located on the cores of the O_b^{q-2} boundary pseudo-ions.¹¹ The coordination of this cluster shareholder to the simplest representative of nitroxides, the H₂NO radical, was analyzed with variation of the following geometric parameters (see Scheme 1): *r*, the distance between the O atom in H₂NO and the Al atom in the LAS; *α* and *φ*, the angles reflecting the extent of pyramidity of the LAS and H₂NO, respectively; and *θ*, the angle reflecting the extent of nonlinearity of the Al—O—N fragment.

Scheme 1



Quantum-chemical SCF MO LCAO calculations of the magnetic-resonance parameters of the paramagnetic SC carried out⁷ in the INDO valence approximation made it possible to conclude that the simple cluster model (see Scheme 1) having the shape of a regular (*α* = 109°28') truncated tetrahedron with variable distance *r* between H₂NO and LAS is quite adequate for a non-contradictory semiquantitative explanation of the whole set of experimental data accumulated so far.²⁻⁵ It was also found that the extent of pyramidity of the

nitroxide ($\varphi \neq 0$) is not as significant as the factor of bending ($\theta \neq 0$) of the resulting adsorption form. In order to study further and to refine the structural parameters characterizing the donor-acceptor binding of nitroxides to the LAS on the Al_2O_3 surface, in the present study we compare the above conclusions based on simplified quantum-chemical analysis⁷ with those made in terms of more perfect quantum-chemical methods (both semiempirical and nonempirical). In addition, in the quantum-chemical calculations we used the so-called covalent model of LAS that is more often encountered in scientific publications.^{12–14}

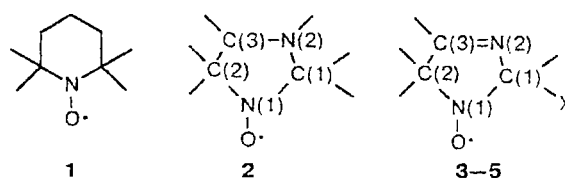
Scheme for the cluster quantum-chemical calculations of the paramagnetic SC on Al_2O_3

In view of the experimentally established² similarity between the magnetic-resonance parameters of the donor-acceptor complexes of nitroxides with AlCl_3 in non-polar solvents and those of the complexes with the surface LAS on Al_2O_3 , the latter were modeled (see Scheme 1) by the covalent (built of atoms¹¹) $\text{Al}(\text{OH})_3$ cluster. This model had been widely tested in non-empirical and semiempirical quantum-chemical calculations for chemisorbed molecular forms.¹⁴ At the same time, it should be taken into account that in those cases¹³ where the covalent and ionic approaches have been compared,¹¹ it was demonstrated that the covalent $[\text{Al}(\text{OH})_3]$ and noncharged ionic $[\text{Al}^{3+}(\text{O}_6^-)_3]$ clusters are equivalent.

In order to test successively various calculation procedures, it is quite natural to carry out initially comparative quantum-chemical analysis of structural, spin, and radiospectroscopic characteristics of the coordination of the covalent cluster LAS, $\text{Al}(\text{OH})_3$, to the simplest representative of nitroxides, viz., the H_2NO radical, and then to pass to objects that have been extensively studied experimentally such as paramagnetic SC formed by probe stable radicals 1–5 (Scheme 2) and the LAS of the alumina surface. All the quantum-chemical calculations were performed using the unrestricted Hartree–Fock (UHF) method; nonempirical calculations were performed in terms of the STO-3G,

STO-6G, 3-21G, and 6-31G basis sets, while semiempirical calculations were carried out using MNDO, AM1, and PM3 parametric versions.¹⁵ For N and Al (A) nuclei, the Hartree–Fock values¹⁶ for the proportionality coefficients between the spin populations ρ_s^A of the valence s-AO and isotropic HFC constants a_{iso}^A were used.

Scheme 2



X = Me (3), Ph (4), C_8H_{17} (5)

Since it is of special interest to evaluate the effect of structural transformations of the LAS and the nitroxide on the magnetic-resonance parameters of the SC formed, the efficiencies of the following models for the complex should be verified. The first structural type of the SC (I) involves the full optimization of the geometry of both the H_2NO radical and the $\text{Al}(\text{OH})_3$ cluster. In this case, quantum-chemical simulation was carried out using all the nonempirical and semiempirical methods mentioned above (Tables 1 and 2).

If we assume that the shape of the tetrahedral aluminum-oxygen fragment in alumina is fairly rigid ("frozen"), we obtain the second structural type of SC (II): in the system, only the geometry of H_2NO is fully optimized, whereas the fixed cluster is shaped like a regular truncated tetrahedron with the length of the Al–O chemical bond in the cluster of 1.82 Å (this is the average value for $\gamma\text{-Al}_2\text{O}_3$ found experimentally from the displacement of Al–K α fluorescence lines¹⁷). The geometric parameters for this structure determined by semiempirical MNDO calculations ($r(\text{Al}–\text{O}) = 1.82$ Å, $r(\text{Al} \cdots \text{O}) = 1.86$ Å, $r(\text{O}–\text{N}) = 1.23$ Å, $r(\text{N}–\text{H}) = 1.02$ Å, $\alpha = 109^\circ$, $\theta = 50^\circ$, $\varphi = 25^\circ$) were used subsequently in the nonempirical calculations of the elec-

Table 1. Structural, magnetic-resonance, and electrostatic parameters of the H_2NO radical calculated by several methods

Parameter	MNDO	AM1	PM3	STO-3G	STO-6G	3-21G	6-31G
$r(\text{O}–\text{N})/\text{\AA}$	1.22	1.22	1.23	1.34	1.34	1.34	1.30
$r(\text{N}–\text{H})/\text{\AA}$	1.01	1.00	0.98	1.02	1.02	0.99	0.99
φ/deg	0.00	0.00	0.00	0.00	0.00	0.00	0.00
$a_{\text{iso}}^{\text{N}}/\text{Oe}$	13.00	15.00	10.00	3.00	3.00	10.00	17.00
$\rho_{\text{N}}^{\text{O}}$	0.45	0.51	0.64	0.10	0.10	0.18	0.24
$\rho_{\text{O}}^{\text{O}}$	0.60	0.54	0.40	0.93	0.93	0.87	0.81
Q^{N}	–0.09	–0.10	0.61	–0.34	–0.35	–0.49	–0.46
Q^{O}	–0.26	–0.31	–0.55	–0.05	–0.05	–0.23	–0.28
$ \mu /\text{D}$	3.00	3.20	3.60	1.70	1.70	2.60	2.90

Table 2. Structural, magnetic-resonance, electrostatic, and energy parameters of the cluster paramagnetic SC, $\text{H}_2\text{NO}\cdots\text{Al}(\text{OH})_3$, found by calculations with full optimization of the geometry using various methods

Parameter	MNDO	AM1	PM3	STO-3G	STO-6G	3-21G	6-31G
$r(\text{Al}-\text{OH})/\text{\AA}$	1.70	1.74	1.76	1.73	1.70	1.70	1.72
$r(\text{Al}\cdots\text{O})/\text{\AA}$	1.95	1.86	1.89	2.09	2.03	1.94	2.00
$r(\text{O}-\text{N})/\text{\AA}$	1.23	1.24	1.27	1.39	1.37	1.31	1.27
$r(\text{N}-\text{H})/\text{\AA}$	1.02	1.01	0.99	1.03	1.03	1.00	1.00
α/deg	100.00	98.00	101.00	97.00	100.00	106.00	106.00
θ/deg	52.00	65.00	72.00	71.00	72.00	63.00	60.00
φ/deg	28.00	20.00	0.00	57.00	66.00	12.00	3.00
$a_{\text{iso}}^{\text{Al}}/\text{Oe}$	-2.00	-2.00	-2.00	-7.00	-8.00	-7.00	-8.00
$a_{\text{iso}}^{\text{N}}/\text{Oe}$	28.00	25.00	13.00	3.00	4.00	27.00	34.00
ρ^{N}	0.48	0.61	0.75	0.02	0.04	0.46	0.51
ρ^{O}	0.52	0.43	0.30	0.98	0.96	0.64	0.59
Q^{Al}	0.95	0.72	0.86	0.87	0.97	1.54	1.90
Q^{N}	0.04	0.01	0.58	-0.27	-0.29	-0.34	-0.31
Q^{O}	-0.20	-0.21	-0.43	-0.01	-0.03	-0.35	-0.44
Q^{R}	0.23	0.29	0.25	0.16	0.13	0.14	0.10
$ \mu /\text{D}$	4.80	4.80	5.10	2.60	2.70	3.70	3.90
$\Delta E_{\text{c}}/\text{kcal mol}^{-1}$	-5.40	-10.80	-25.00	-21.70	-21.30	-32.60	-19.00

Table 3. Structural, magnetic-resonance, electrostatic, and energy parameters of the cluster paramagnetic SC, $\text{H}_2\text{NO}\cdots\text{Al}(\text{OH})_3$, with "frozen" LAS calculated by various methods

Parameter	MNDO	AM1	PM3	STO-3G	STO-6G	3-21G	6-31G
$r(\text{Al}-\text{OH})/\text{\AA}$	1.82	1.82	1.82	1.82	1.82	1.82	1.82
$r(\text{Al}\cdots\text{O})/\text{\AA}$	1.86	1.84	1.86	1.86	1.86	1.86	1.86
$r(\text{O}-\text{N})/\text{\AA}$	1.23	1.24	1.26	1.23	1.23	1.23	1.23
$r(\text{N}-\text{H})/\text{\AA}$	1.02	1.01	0.98	1.02	1.02	1.02	1.02
α/deg	109.00	109.00	109.00	109.00	109.00	109.00	109.00
θ/deg	50.00	67.00	71.00	50.00	50.00	50.00	50.00
φ/deg	25.00	1.00	4.00	25.00	25.00	25.00	25.00
$a_{\text{iso}}^{\text{Al}}/\text{Oe}$	-3.00	-2.00	-2.00	-10.00	-10.00	-5.00	-5.00
$a_{\text{iso}}^{\text{N}}/\text{Oe}$	27.00	19.00	13.00	19.00	19.00	34.00	4.00
ρ^{N}	0.54	0.61	0.75	0.33	0.32	0.59	0.65
ρ^{O}	0.48	0.43	0.30	0.74	0.74	0.52	0.46
Q^{Al}	0.89	0.65	0.82	0.77	0.82	1.36	1.72
Q^{N}	0.05	-0.03	0.66	-0.26	-0.28	-0.27	-0.25
Q^{O}	-0.19	-0.19	-0.42	-0.06	-0.07	-0.41	-0.50
Q^{R}	0.29	0.33	0.30	0.22	0.22	0.20	0.14
$ \mu /\text{D}$	7.50	7.10	7.30	6.30	6.30	7.70	7.80
$\Delta E_{\text{c}}/\text{kcal mol}^{-1}$	-24.50	-21.60	-36.30	-29.40	-30.80	-51.80	-41.50

tronic structure of the SC, its HFC constants, and spin and electron populations (Table 3).

The third structural type of the model SC (III) differs from the second type in that the Al atom in the $\text{Al}(\text{OH})_3$ cluster is regarded as mobile, *i.e.*, it is involved in the procedure of geometric optimization together with the H_2NO radical. The conclusions preceding this simulation (see below) account for the fact that the quantum-chemical calculations of the structure and properties of this complex were carried out in terms of only semiempirical methods (Table 4).

Similarly, in terms of the MNDO approximation, the calculations for free nitroxides 1–5 (see Scheme 2) and for their SC (Schemes 3 and 4) with the cluster

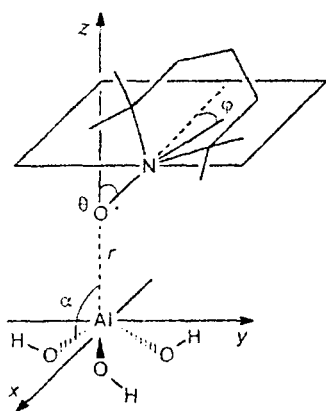
LAS, $\text{Al}(\text{OH})_3$, were carried out (Tables 5–10). In this case, as in the case of the above-described $\text{H}_2\text{NO}\cdots\text{Al}(\text{OH})_3$ simplified coordination system, we analyzed the structural and radiospectroscopic characteristics of the donor-acceptor binding of nitroxides to the model $\text{Al}(\text{OH})_3$ cluster, whose geometry was either fully optimized (structural type I) or considered to be "frozen" (structural type II). Owing to the similarity of the accomplished quantum-chemical calculations for the model paramagnetic SC (see Schernes 1, 3, and 4), the results obtained make it possible to judge on the efficiency of the application of the simplified cluster model to the analysis of the experimentally established features

Table 4. Structural, magnetic-resonance, electrostatic, and energy parameters of the paramagnetic SC, $\text{H}_2\text{NO}\cdots\text{Al}(\text{OH})_3$, with mobile Al atom calculated by semiempirical methods

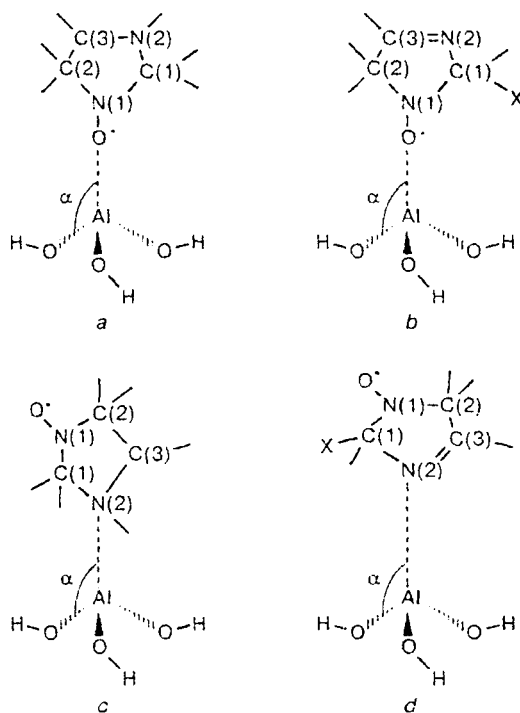
Parameter	MNDO	AM1	PM3
$r(\text{Al}-\text{OH})/\text{\AA}$	1.74	1.75	1.78
$r(\text{Al}\cdots\text{O})/\text{\AA}$	1.98	1.87	1.90
$r(\text{O}-\text{N})/\text{\AA}$	1.23	1.23	1.26
$r(\text{N}-\text{H})/\text{\AA}$	1.02	1.01	0.99
α/deg	103.00	102.00	105.00
θ/deg	46.00	61.00	71.00
φ/deg	25.00	10.00	4.00
$a_{\text{iso}}^{\text{Al}}/\text{Oe}$	-0.50	0.00	-1.50
$a_{\text{iso}}^{\text{N}}/\text{Oe}$	27.00	20.00	13.00

Parameter	MNDO	AM1	PM3
ρ^{N}	0.51	0.63	0.74
ρ^{O}	0.50	0.43	0.30
Q^{Al}	0.89	0.73	0.85
Q^{N}	0.04	-0.03	0.65
Q^{O}	-0.24	-0.24	-0.44
Q^{R}	0.20	0.25	0.25
$ \mu /\text{D}$	10.90	10.40	10.50
$\Delta E_e/\text{kcal mol}^{-1}$	2.30	0.10	-5.90
$i_{\text{O}-\text{N}}(\%)$	0.20	-3.40	-8.30
$i_{\text{N}-\text{H}}(\%)$	-3.50	-2.90	-2.60

Scheme 3



Scheme 4



of the coordination of nitroxide probes to the surface LAS on alumina.

Results and Discussion

Cluster paramagnetic SC $\text{H}_2\text{NO}\cdots\text{Al}(\text{OH})_3$. Table 1 lists the lengths of the O—N and N—H bonds, the φ angles (see Scheme 1), the constants $a_{\text{iso}}^{\text{N}}$ of the isotropic HFC with the ^{14}N nuclei, the electrical dipole moments $|\mu|$, the charges Q , and the total spin populations ρ of the N and O atoms in the H_2NO radical found by semiempirical and nonempirical methods. It can be seen from the data of Table 1 that the O—N bond lengths calculated by semiempirical MNDO, AM1, and PM3 methods differ insignificantly, and the values calculated by nonempirical methods are also close to one another; however, the latter are markedly larger than those found by semiempirical calculations and also than the reliable reported values ($r(\text{O}-\text{N}) = 1.2$ to 1.3 Å) for most of nitroxides.^{1,6} The $r(\text{N}-\text{H})$ distance is virtually insensitive to the choice of the particular calculation scheme (~ 1.0 Å).

Since the experimental isotropic HFC constants $a_{\text{iso}}^{\text{N}}$ for nitroxides are normally 13–17 Oe,^{2–5} the structural data obtained by MNDO, AM1, and UHF/6-31G methods are the most reliable. The PM3 and UHF/3-21G procedures somewhat underestimate these constants, and simpler nonempirical schemes, STO-3G and STO-6G, describe them inadequately. According to MNDO and AM1 methods, the total spin population of the O atom (ρ^{O}) is somewhat higher than that of the N atom (ρ^{N}); this is in agreement with the $\rho^{\text{O}} : \rho^{\text{N}}$ ratio estimated empirically, viz., 0.6 : 0.4.¹ In terms of the PM3 procedure, this ratio is inverted, and all of the nonempirical methods markedly overestimate the spin population of the O atom.

The calculated Q^N and Q^O values on the N and O atoms in the H_2NO radical depend substantially on the calculation procedure used. Note that only the PM3 approximation predicts a large positive charge on the N atom, whereas in terms of other methods, this atom is described as carrying a negative charge. The results obtained by semiempirical MNDO and AM1 methods indicate that the negative charge on the O atom is larger than that on the N atom, whereas nonempirical calculations lead to the opposite ratio.

The electrical dipole moment of the H_2NO radical found by semiempirical calculations is normally larger in magnitude than that found by nonempirical procedures. However, it should be emphasized that the values obtained by MNDO and UHF/6-31G calculations are virtually identical. Thus, the data listed in Table 1 indicate that the semiempirical MNDO and AM1 methods can apparently represent the whole set of structural, electronic, and magnetic-resonance parameters characterizing the class of nitroxide probes even more adequately than the standard nonempirical methods.

Table 2 lists the calculated lengths of the $r(Al-O)$, $r(Al...O)$, $r(O-N)$, and $r(N-H)$ bonds, the α , θ , and ϕ angles (see Scheme 1), the a_{iso}^N and a_{iso}^O constants, the total spin populations of the N (p^N) and O (p^O) atoms, the charges on Al (Q^Al), N (Q^N), and O (Q^O) atoms, excessive charges Q^R on the H_2NO radical fragment, the dipole moments $|\mu|$, and the energies ΔE_c of the formation of the cluster paramagnetic SC, $H_2NO...Al(OH)_3$, with a fully optimized geometry. Now we consider the results of nonempirical calculations for this SC (see Table 2).

The intra-cluster $r(Al-O)$ distance determined by nonempirical methods is markedly smaller than this distance in an alumina crystal found experimentally ($r(Al-O) \cong 1.82$ Å). The length of the $Al...O$ coordination bond does not depend significantly on the basis set and amounts to ~ 2 Å, which is in agreement with the conclusions made previously.⁷ According to X-ray diffraction results,¹ the O—N bond length in most nitroxides lies in the range of 1.23–1.30 Å. Thus, the $r(O-N)$ distance found by STO-3G, STO-6G, and UHF/3-21G calculations is markedly overestimated. The calculated length of the N—H bond is ~ 1 Å in all cases.

According to the UHF/3-21G and UHF/6-31G methods, the α angle in the $H_2NO...Al(OH)_3$ cluster SC (see Scheme 1) barely differs from the tetrahedral angle, whereas in the STO-3G and STO-6G variants, it is substantially smaller, *i.e.*, the structure of the LAS is flattened. The large magnitude of the θ angle indicates that the H_2NO radical is adsorbed on the alumina surface forming a nonlinear structure. Since the experimental value of the angle (ϕ) characterizing the pyramidity of the N atom in adsorbed nitroxides^{1,6} normally does not exceed 30°, one can assume that the STO-3G and STO-6G methods (see Table 2) tend to overestimate substantially the change in this angle caused by coordination.

For temperatures of 570–1070 K, the constant of isotropic HFC with ^{27}Al is known^{2–5} to lie in the range of 9.0–11.5 Oe; all the corresponding values found by nonempirical methods are in good agreement with these data (see Table 2). On the other hand, the experimental constants of isotropic HFC with the N nucleus in donor-acceptor complexes of nitroxides with $AlCl_3$ are normally close to 19 Oe;^{2,3} the values found by the UHF/3-21G and UHF/6-31G methods are somewhat overestimated, whereas those calculated by the STO-3G and STO-6G procedures are, conversely, markedly underestimated. The advantage of the UHF/3-21G and UHF/6-31G methods in this case was also manifested in the fact that they provided a correct qualitative representation of the experimentally observed increase in the spin population of the N atom in the adsorption SC with respect to that in a separate nitroxide.

The calculated positive charge on the aluminum atom Q^Al depends appreciably on the basis set used (see Table 2); however, in all cases, it is fairly large. All the four nonempirical methods give similar estimates for the charge on the N atom in the cluster SC, *viz.*, approximately -0.3 . It is noteworthy that the STO-3G and STO-6G calculations lead to a nearly zero charge on the O atom in the H_2NO radical fragment. The excessive positive charge on this fragment ($Q^R = 0.10$ to 0.16) found by nonempirical calculations indicates in all cases that the electron density shifts from the nitroxide to the model LAS. The high dipole moment of the cluster SC ($|\mu| = 2.6$ to 3.9 D) also attests to a substantial redistribution of the electron density.

Thus, the analysis of the results of nonempirical calculations presented in Table 2 indicates that in the estimation of the O—N bond length, the ϕ angle, the constants of isotropic HFC with ^{14}N , and the total spin populations of the N and O atoms, the UHF/3-21G and UHF/6-31G procedures provide better agreement with the experimental results than the STO-3G and STO-6G procedures. However, it is noteworthy that the energy of complex formation predicted by the latter differs only slightly from that calculated in terms of the UHF/3-21G method.

According to semiempirical MNDO, AM1, and PM3 methods, as also the nonempirical methods (see Table 2), the $Al-O$ intra-cluster bond in the SC with a fully optimized geometry proved to be shorter than this bond in alumina found experimentally (1.82 Å). The $r(Al...O)$ distances outside the cluster obtained within the framework of the AM1 and PM3 methods are markedly smaller than those found by nonempirical methods or using the MNDO approximation. The O—N bond length is represented adequately by all the semiempirical methods but not by nonempirical methods (STO-3G, STO-6G, and UHF/3-21G).

According to all the semiempirical approximations, the α angle characterizing the extent of pyramidity of the model LAS is markedly smaller than the tetrahedral angle (see Table 2) and is close to that found by the

STO-3G and STO-6G nonempirical schemes. Although the θ angle calculated in terms of MNDO is the smallest in the series of these values, it indicates unambiguously that the AION fragment in the cluster SC formed is markedly nonlinear (see Scheme 1). The estimates of the ϕ angle in this SC provided by all the semiempirical methods (see Table 2) are quite adequate.

The constant of isotropic HFC with the aluminum nucleus $a_{\text{iso}}^{\text{Al}}$ in the cluster paramagnetic SC with a fully optimized geometry is poorly represented in terms of the semiempirical methods that we used; this is due to the large errors in the calculations of low spin densities. At the same time, in general, these methods are better in predicting $a_{\text{iso}}^{\text{N}}$ than the nonempirical procedures. All three semiempirical methods indicate that the total spin population of the N atom in the cluster SC is higher than that in the free radical (see Table 2), which is consistent with experimental results.²⁻⁴ Unlike the nonempirical schemes used (especially STO-3G and STO-6G), the semiempirical MNDO, AM1, and PM3 approximations do not tend to overestimate the total spin population of the O atom in this SC.

The charges on the Al atom in the cluster SC with a fully optimized geometry estimated by semiempirical methods as well as by the STO-3G and STO-6G nonempirical procedures are close to one another and are slightly less than 1. However, the charges on the nitrogen atom Q^{N} found in terms of the MNDO, AM1, and PM3 methods are always positive, unlike those calculated nonempirically. As in the case of free H_2NO radical, in this case, too, the maximum magnitude of $|Q^{\text{N}}|$ is obtained in the parametric PM3 version. According to all the semiempirical approximations, the negative charge Q^{O} on the O atom is relatively large, and the excessive positive charge Q^{R} on the H_2NO radical fragment of the cluster SC is much larger than that found in nonempirical schemes (see Table 2). The dipole moments calculated by MNDO, AM1, and PM3 markedly exceed those calculated nonempirically, thus reflecting a substantially larger extent of the electron transfer from the radical to the cluster LAS. It should be noted that the energy of complex formation ΔE_{c} varies over a fairly wide range (from -5 to -25 kcal mol $^{-1}$) on going from one semiempirical version to another; in the case of nonempirical approaches, this range is not so wide.

Thus, comparative analysis of the results presented in Table 2 indicates that in general, semiempirical approaches are not less efficient than nonempirical methods, and in the estimation of the length of the O—N bond and the isotropic HFC constant with the N nucleus in the cluster paramagnetic SC, they can be even more adequate. Owing to this fact, together with the fact that these methods require much less computer time, the subsequent (see below) consideration of the structural and radiospectroscopic characteristics of the coordination of the more complex nitroxide probes to the surface LAS of alumina was performed using only semiempirical methods. Preference was given to the MNDO approxi-

mation, because it has been tested most widely^{15,18-21} in the quantum-chemical calculations of thermodynamic, structural, and magnetic-resonance properties of organic and inorganic free radicals.

The values listed in Table 3 differ from the data of Table 2 in that they correspond to a partial rather than full optimization of the geometry of the same cluster SC, $\text{H}_2\text{NO}\cdots\text{Al}(\text{OH})_3$. In this case, only geometric parameters related to the radical subsystem (H_2NO) were optimized, whereas the structure of the cluster LAS $\text{Al}(\text{OH})_3$ was considered to be "frozen" as a regular ($\alpha = 109^\circ$) truncated tetrahedron in which the length of the intra-cluster Al—O chemical bond is equal to the value found experimentally (1.82 Å).¹⁷ From a comparison of the data listed in Tables 2 and 3, it follows that the rigid structural fixation of the cluster does not cause any significant changes in the geometry of the coordinated H_2NO radical, although the $r(\text{Al}\cdots\text{O})$ interatomic distance outside the cluster proved to be markedly shorter in this case.

All the methods that we used (both nonempirical and semiempirical) indicate that the constant of isotropic HFC with the Al nucleus in the paramagnetic SC (see Scheme 1) is relatively insensitive to the optimization of the geometry of the cluster LAS (see Tables 2 and 3). At the same time, the $a_{\text{iso}}^{\text{N}}$ constant found nonempirically has markedly increased in all cases (especially in the STO-3G and STO-6G versions), whereas according to the semiempirical approximations, it either remained the same (MNDO, PM3) or decreased (AM1). The total spin population ρ^{O} of the O atom in the H_2NO radical fragment calculated in terms of the STO-3G and STO-6G schemes is substantially overestimated, in view of the fact that all the other methods predict an inverse ratio, $\rho^{\text{O}} < \rho^{\text{N}}$.

All the calculation techniques without exception indicate that the charge Q^{Al} on the Al atom decreases as a result of fixation of the structure of the cluster LAS in the paramagnetic SC (see Tables 2 and 3). However, nonempirical and semiempirical approaches lead to qualitatively different results concerning the character of variation of Q^{N} and Q^{O} . Nevertheless, both approaches predict quantitatively nearly equal extents of the increase in the electron transfer ($\delta Q^{\text{R}} \approx 0.05$) from the coordinated radical to the cluster LAS, and the difference between the dipole moments of the paramagnetic SC found semiempirically and nonempirically, in general, markedly decreases.

Special attention should be paid to the fact that the rigid fixation of the structure of the cluster LAS (both isolated and incorporated in the paramagnetic SC) taken from experimental results changed substantially (by up to ~ 20 kcal mol $^{-1}$) the earlier estimates of ΔE_{c} ; strange as it may seem, in the case of the MNDO, AM1, and UHF/6-31G methods, their agreement with the experimental results found for related compounds² became much better. In addition, as has been emphasized above, the ratio of the total spin populations, $\rho^{\text{N}} > \rho^{\text{O}}$, also

became consistent with that observed by ESR for several coordinated nitroxides.^{2–5} Similar results that can arise criticism, have repeatedly attracted attention^{16,19–21} in connection with the insufficient adequacy of the methods used for the energy optimization of the geometries of paramagnetic systems (with open electronic shells).

Table 4 presents characteristics that differ from the corresponding values listed in Table 3 in that they relate to the equilibrium structures found without placing any limitations on the mobilities of not only the H₂NO radicals but also the Al atom in the cluster LAS (both isolated and incorporated in the paramagnetic SC). In addition, the i_{A-B} indices²² characterizing the changes in the strengths of the chemical bonds in the H₂NO radical following its coordination are also included in Table 4. These indices correlate well with the increments of the N—O and N—H bond lengths as follows from a comparison of the $r(N-O)$ and $r(N-H)$ values in Tables 1 and 4.

The structural parameters obtained with the mobile Al atom in the cluster paramagnetic SC (see Table 4) do not differ markedly from those obtained by calculations with the full optimization of its geometry (see Table 2); this can be easily followed by comparing the corresponding interatomic distances and angles. It should be emphasized that the flattening of the cluster LAS, which has also been observed previously in similar quantum-chemical studies,²³ is much less pronounced in the case where the intra-cluster environment of the mobile Al atom is rigidly fixed. However, it is noteworthy that, despite the fact that the corresponding structural and electronic characteristics listed in Tables 2 and 4 are close, the electrical dipole moments differ more than twofold.

The transition of the "frozen" LAS (see Table 3) to its structurally flexible form with a mobile Al atom (see Table 4) has almost no effect on the a_{iso}^N values or on the spin populations ρ^N and ρ^O ; however, the a_{iso}^{Al} constant becomes even smaller and the energies of complex formation ΔE_c found in the MNDO and AM1 approximations are absolutely inadequate. Therefore, in the quantum-chemical simulation of the radical adsorption on Al₂O₃, it is more reasonable to fix rigidly the structure of the cluster LAS based on crystallographic and other physicochemical data than to determine it using methods of energy optimization. It should be emphasized that this is also indicated by the results of a similar quantum-chemical calculation carried out previously⁷ using noncharged ionic cluster models.

Cluster paramagnetic SC of tanane with Al(OH)₃

When tanane is adsorbed on the alumina surface, two types of strong LAS are manifested yielding magnetically nonequivalent SC. It is conventional^{2–5} to identify the first type of LAS as three-coordinate Al³⁺ ions. At 570–1070 K, the constant of isotropic HFC with the ²⁷Al nucleus lies in the 9.0–11.7 Oe range, and that with the ¹⁴N nucleus is close to 20 Oe. The magnetic-resonance parameters of the resulting SC depend appreciably

Table 5. Structural, magnetic-resonance, electrostatic, and energy parameters of tanane and its SC with the model cluster LAS, Al(OH)₃

Parameter	Tanane	SC I	SC II
$r(Al-OH)/\text{\AA}$	—	1.70	1.82
$r(Al...O)/\text{\AA}$	—	1.98	1.86
$r(O-N)/\text{\AA}$	1.23	1.23	1.23
$r(N-C)/\text{\AA}$	1.53	1.54	1.55
α/deg	—	100.00	109.00
θ/deg	—	22.00	25.00
φ/deg	19.00	18.00	17.00
a_{iso}^{Al}/Oe	—	−1.00	−1.00
a_{iso}^N/Oe	20.00	22.00	22.00
ρ^N	0.40	0.61	0.60
ρ^O	0.59	0.41	0.42
Q^{Al}	—	0.99	0.95
Q^N	−0.10	0.02	−0.01
Q^O	−0.28	−0.31	−0.31
Q^R	0.00	0.17	0.25
$ \mu /D$	3.00	7.30	9.90
$\Delta E_c/\text{kcal mol}^{-1}$	—	−18.70	−33.80
$i_{O-N}(\%)$	—	1.60	1.30
$i_{N-C}(\%)$	—	−3.30	−4.60

ably on the conditions of training of the alumina samples.

The structural, radiospectroscopic, electrostatic, and energy parameters found by the MNDO-UHF semi-empirical method for tanane and its SC (see Scheme 3) with the model cluster LAS, whose geometry was either fully optimized (SC I) or considered to be "frozen" (SC II), are summarized in Table 5. Comparative analysis of the values listed in Table 5 indicates that the calculated length of the O—N bond in tanane (1.23 Å) is virtually identical to that in the simplest nitroxide H₂NO. The φ angle is close to 20°, which is in good agreement with the data reported for nitroxides related to tanane.^{1,6} The a_{iso}^N constant (20 Oe) differs insignificantly from that found for tanane by ESR (16 Oe), and the $\rho^O : \rho^N \approx 0.6 : 0.4$ ratio is also consistent with the published data.^{1,4}

In the paramagnetic SC I, as in its model analog, H₂NO...LAS, the intra-cluster Al—O bond is markedly shorter than the average $r(Al-O)$ distance in alumina, while the length of the N—O bond is insensitive to the coordination. The $r(Al...O)$ interatomic distance and the α angle in SC I (see Table 5) are also nearly identical with those in the similar H₂NO...LAS structure (see Table 2). Thus, the replacement of H₂NO by tanane has no effect on the optimized geometry of the cluster LAS in the resulting paramagnetic SC.

However, the θ angle in SC I is much smaller than that in the similar H₂NO...LAS system. This is caused by the sharp increase in steric hindrance in this complex due to the presence of four methyl groups in tanane. The extent of pyramidalicity of the N atom measured by the φ angle in SC I is nearly the same as that in the tanane itself and is in agreement with experimental data.^{1,6}

The $a_{\text{iso}}^{\text{Al}}$ constant of isotropic HFC with the Al nucleus found by MNDO for SC I is an order of magnitude smaller than the experimental value²⁻⁵ but virtually coincides with that calculated previously⁷ in the INDO approximation. This underestimation of the $a_{\text{iso}}^{\text{Al}}$ value is mostly due to the fact that the spin densities on the Al nuclei are relatively small (~ 0.01) and, as a consequence, the errors in calculations of these values by approximate methods are large. At the same time, the $a_{\text{iso}}^{\text{N}} \approx 22$ Oe constant is in good agreement with experimental results.⁴

The total spin populations of the N and O atoms in the paramagnetic SC I indicate that the $\rho^{\text{O}} : \rho^{\text{N}}$ ratio has been inverted. In this case, the excess of electrons on the O atom is much larger than that in the $\text{H}_2\text{NO} \dots \text{LAS}$ cluster optimized in a similar way (cf. Tables 2 and 4), while the electron deficiency on the N and Al atoms is virtually the same. When H_2NO is replaced by tanane, the extent of electron transfer from the radical to the cluster LAS in the paramagnetic SC I hardly changes, whereas its electrical dipole moment increases approximately twofold.

The experimentally estimated energy of the formation of the donor-acceptor complexes of tanane with the surface LAS of alumina is known² to lie in the range of 32–35 kcal mol⁻¹. It follows from the data listed in Table 5 that the ΔE_c value (SC I) calculated with full optimization of all the geometric parameters is much smaller than the experimental value. Nevertheless, this value undoubtedly points to a chemisorption mechanism of the interaction of tanane with LAS on the Al_2O_3 surface.

In the paramagnetic SC II with the "frozen" cluster LAS, the O–N and N–C bond lengths, the θ and φ angles, the constants of isotropic HFC $a_{\text{iso}}^{\text{Al}}$ and $a_{\text{iso}}^{\text{N}}$, the total spin populations ρ^{N} and ρ^{O} , and the atomic charges Q^{Al} , Q^{N} , and Q^{O} calculated by MNDO are nearly identical with those found for SC I with a fully optimized geometry (see Table 5). However, the $r(\text{Al} \dots \text{O})$ interatomic distance outside the cluster for SC II is much shorter and the α angle is larger than those in SC I, which was also manifested in the simplified $\text{H}_2\text{NO} \dots \text{LAS}$ model calculated in a similar way. At the same time, on going from SC I to SC II, the excessive charge on the radical and the dipole moment increase indicating an increase in the extent of electron transfer from tanane to the cluster LAS.

In the formation of paramagnetic SC II, the O–N bond becomes slightly stronger ($i_{\text{O-N}} = 1.3\%$), while the N–C bond becomes weaker ($i_{\text{N-C}} = -4.6\%$). The energy of the coordination of tanane to the "frozen" cluster LAS found by MNDO is in good agreement with the experimental value (32–35 kcal mol⁻¹). This is an additional argument in favor of the rigid fixation of the geometry of the cluster LAS in the quantum-chemical simulation of the chemisorption of nitroxide probes on the surface of Al_2O_3 .

Cluster paramagnetic SC formed by imidazoline and imidazolidine nitroxides with $\text{Al}(\text{OH})_3$. Characteristic

structures and ample possibilities for varying the substituents make nitroxides of the imidazoline and imidazolidine series more sensitive to the specific features of the oxide surface than tanane. These radicals are used successfully to study experimentally at the molecular level the structures of adsorption complexes formed on oxide catalysts and to establish the structures of the surface active sites as well as the orientations and mobilities of coordinated paramagnetic species.³ The constants of isotropic HFC with ^{14}N in these radicals are equal to ~ 14 – 15 Oe^{3,24} (depending on the structure and the chemical nature of the environment), i.e., they are smaller than that for tanane.

The special interest in the radiospectroscopic studies of this type of radicals is caused by the fact that they incorporate two (see Scheme 2) electron-donating sites (the N(2) and O atoms) that compete in the coordination to the surface aluminum ions (see Scheme 4). The preferred coordination by a particular site is largely determined by the structure of the radical and can be detected experimentally^{3,4} based on the ESR spectral pattern and on the magnitude of the constant of HFC with the $^{14}\text{N}(1)$ nucleus in the resulting SC. For example, radical 2 is coordinated only through the O atom, whereas 3 binds through the N(2) atom. In the case of radicals 4 and 5, superposition of the ESR spectra is observed indicating that these species can be coordinated to the LAS through both the N(2) and O atoms.

Table 6 presents the structural, magnetic-resonance, and electrostatic parameters of free radicals 2–5 calculated by the semiempirical MNDO-UHF method. It is of interest to compare these radicals with one another and with tanane (see Table 5). It can be seen from the data given in Tables 5 and 6 that the N–O bond lengths and the similar $r(\text{N} \dots \text{C})$ interatomic distances in noncoordinated radicals 1–5 differ only slightly. However, the extent of pyramidity of the N(1) atom in all of the imidazoline and imidazolidine radicals is less than that in tanane. It is noteworthy that the constant of

Table 6. Structural, magnetic-resonance, and electrostatic parameters of radicals 2–5

Parameter	2	3	4	5
$r(\text{O} \dots \text{N}(1))/\text{\AA}$	1.22	1.22	1.22	1.22
$r(\text{N}(1) \dots \text{C}(1))/\text{\AA}$	1.52	1.52	1.54	1.52
$r(\text{N}(1) \dots \text{C}(2))/\text{\AA}$	1.51	1.53	1.53	1.53
$r(\text{N}(2) \dots \text{C}(1))/\text{\AA}$	1.48	1.47	1.47	1.47
$r(\text{N}(2) \dots \text{C}(3))/\text{\AA}$	1.48	1.30	1.30	1.30
φ/deg	14.00	17.00	18.00	12.00
$a_{\text{iso}}^{\text{N}(1)}/\text{Oe}$	19.00	19.00	20.00	18.00
$\rho^{\text{N}(1)}$	0.42	0.40	0.41	0.42
ρ^{O}	0.59	0.59	0.59	0.59
$Q^{\text{N}(1)}$	-0.11	-0.12	-0.11	-0.13
$Q^{\text{N}(2)}$	-0.45	-0.23	-0.22	-0.23
Q^{O}	-0.26	-0.25	-0.26	-0.25
$ \mu /\text{D}$	2.90	2.50	2.40	2.50

isotropic HFC with the $^{14}\text{N}(1)$ nucleus and the φ angle vary in parallel, *i.e.*, the conclusion that this angle plays only a minor role⁷ drawn using a simpler model is not completely confirmed.

The fact that the $a_{\text{iso}}^{\text{N}(1)}$ constants for free radicals 2, 3, and 5 (see Table 6) are smaller than that for tanane is consistent with the regularities established experimentally.^{3,24} As in tanane, the $\rho^{\text{O}} : \rho^{\text{N}}$ ratio of spin populations in paramagnetic species 2–5 is approximately 0.6 : 0.4, which is apparently typical of the class of nitroxides.

The calculated charges on the O and N(1) atoms in radicals 2–5 are virtually identical and barely differ from those found for tanane. The large difference between the charges on the N(2) atom found for imidazoline and imidazolidine radicals (see Table 6) is most of all due to the dissimilar hybrid valence states of this atom. Among noncoordinated species 1–5, tanane (see Table 5) and radical 2 possess the largest dipole moments exceeding the rest of the values given in Table 6 by ~0.5 D. This indicates unambiguously that specific features of the ring exert a markedly stronger effect on the main characteristics of free nitroxides than the variation of substituents.

Now we consider the results of quantum-chemical calculations (see Tables 7–10) for the coordination of

Table 8. Structural, magnetic-resonance, electrostatic, and energy parameters of the SC formed by radicals 2–5 with the "frozen" cluster LAS, $\text{Al}(\text{OH})_3$, (coordination through the O atom)

Parameter	2	3	4	5
$r(\text{Al}\cdots\text{O})/\text{\AA}$	1.86	1.86	1.86	1.86
$r(\text{O}-\text{N}(1))/\text{\AA}$	1.23	1.23	1.22	1.23
$r(\text{N}(1)-\text{C}(1))/\text{\AA}$	1.53	1.55	1.55	1.55
$r(\text{N}(1)-\text{C}(2))/\text{\AA}$	1.52	1.53	1.53	1.53
$r(\text{N}(2)-\text{C}(1))/\text{\AA}$	1.47	1.46	1.47	1.46
$r(\text{N}(2)-\text{C}(3))/\text{\AA}$	1.48	1.30	1.30	1.30
θ/deg	35.00	37.00	32.00	37.00
φ/deg	15.00	13.00	13.00	15.00
$a_{\text{iso}}^{\text{Al}}/\text{Oe}$	-0.1	-0.5	-1.4	-0.1
$a_{\text{iso}}^{\text{N}(1)}/\text{Oe}$	21.00	22.00	22.00	21.00
$\rho^{\text{N}(1)}$	0.62	0.61	0.61	0.62
ρ^{O}	0.40	0.42	0.44	0.40
Q^{Al}	0.94	0.93	0.93	0.93
$Q^{\text{N}(1)}$	0.01	-0.02	-0.03	-0.02
$Q^{\text{N}(2)}$	-0.45	-0.23	-0.22	-0.23
Q^{O}	-0.28	-0.26	-0.26	-0.27
Q^{R}	0.26	0.26	0.25	0.26
$ \mu /\text{D}$	9.50	9.10	8.80	8.80
$\Delta E_c/\text{kcal mol}^{-1}$	-29.50	-29.40	-29.80	-30.50
$i_{\text{O}-\text{N}(1)}(\%)$	0.60	0.70	1.80	0.40
$i_{\text{N}(1)-\text{C}(1)}(\%)$	-4.40	-4.90	-5.00	-5.70
$i_{\text{N}(1)-\text{C}(2)}(\%)$	-3.80	-2.60	-2.40	-3.70
$i_{\text{N}(2)-\text{C}(1)}(\%)$	-0.20	-0.10	-0.20	-0.20
$i_{\text{N}(2)-\text{C}(3)}(\%)$	-0.10	-0.00	-0.10	-0.10

Table 7. Structural, magnetic-resonance, electrostatic, and energy parameters of the SC formed by radicals 2–5 with the model cluster LAS, $\text{Al}(\text{OH})_3$, (coordination through the O atom) calculated with full optimization of the geometry

Parameter	2	3	4	5
$r(\text{Al}-\text{OH})/\text{\AA}$	1.70	1.70	1.70	1.70
$r(\text{Al}\cdots\text{O})/\text{\AA}$	1.97	1.97	1.98	1.98
$r(\text{O}-\text{N}(1))/\text{\AA}$	1.23	1.22	1.22	1.22
$r(\text{N}(1)-\text{C}(1))/\text{\AA}$	1.53	1.54	1.54	1.55
$r(\text{N}(1)-\text{C}(2))/\text{\AA}$	1.52	1.53	1.53	1.53
$r(\text{N}(2)-\text{C}(1))/\text{\AA}$	1.48	1.47	1.47	1.47
$r(\text{N}(2)-\text{C}(3))/\text{\AA}$	1.48	1.30	1.30	1.30
α/deg	100.00	100.00	100.00	100.00
θ/deg	34.00	29.00	23.00	31.00
φ/deg	17.00	14.00	14.00	16.00
$a_{\text{iso}}^{\text{Al}}/\text{Oe}$	-0.10	-0.60	-0.40	-0.40
$a_{\text{iso}}^{\text{N}(1)}/\text{Oe}$	21.00	22.00	21.00	21.00
$\rho^{\text{N}(1)}$	0.56	0.54	0.55	0.55
ρ^{O}	0.44	0.48	0.50	0.47
Q^{Al}	0.98	0.98	0.99	0.98
$Q^{\text{N}(1)}$	-0.01	-0.05	-0.07	-0.04
$Q^{\text{N}(2)}$	-0.45	-0.23	-0.22	-0.23
Q^{O}	-0.26	-0.26	-0.27	-0.27
Q^{R}	0.18	0.18	0.17	0.16
$ \mu /\text{D}$	6.70	6.40	6.10	6.30
$\Delta E_c/\text{kcal mol}^{-1}$	-15.90	-16.80	-17.30	-17.90
$i_{\text{O}-\text{N}(1)}(\%)$	0.80	0.90	2.00	0.90
$i_{\text{N}(1)-\text{C}(1)}(\%)$	-3.60	-4.30	-4.50	-5.20
$i_{\text{N}(1)-\text{C}(2)}(\%)$	-3.30	-2.00	-1.50	-2.70
$i_{\text{N}(2)-\text{C}(1)}(\%)$	-0.10	-0.10	-0.10	-0.10
$i_{\text{N}(2)-\text{C}(3)}(\%)$	-0.10	0.00	0.00	0.00

Table 9. Structural, magnetic-resonance, electrostatic, and energy parameters of the SC formed by radicals 3–5 with the model cluster LAS, $\text{Al}(\text{OH})_3$, (coordination through the N atom) calculated with full optimization of the geometry

Parameter	3	4	5
$r(\text{Al}-\text{OH})/\text{\AA}$	1.70	1.70	1.70
$r(\text{Al}\cdots\text{N}(2))/\text{\AA}$	2.10	2.11	2.12
$r(\text{O}-\text{N}(1))/\text{\AA}$	1.22	1.22	1.22
$r(\text{N}(1)-\text{C}(1))/\text{\AA}$	1.53	1.53	1.53
$r(\text{N}(1)-\text{C}(2))/\text{\AA}$	1.51	1.52	1.52
$r(\text{N}(2)-\text{C}(1))/\text{\AA}$	1.49	1.49	1.50
$r(\text{N}(2)-\text{C}(3))/\text{\AA}$	1.31	1.31	1.31
α/deg	100.00	102.00	103.00
$a_{\text{iso}}^{\text{N}(1)}/\text{Oe}$	19.00	19.00	19.00
$\rho^{\text{N}(1)}$	0.38	0.40	0.39
ρ^{O}	0.60	0.61	0.60
Q^{Al}	0.94	0.93	0.94
$Q^{\text{N}(1)}$	-0.12	-0.13	-0.12
$Q^{\text{N}(2)}$	-0.23	-0.23	-0.24
Q^{O}	-0.23	-0.23	-0.24
Q^{R}	0.22	0.22	0.22
$ \mu /\text{D}$	4.00	3.80	4.00
$\Delta E_c/\text{kcal mol}^{-1}$	-17.10	-16.00	-17.40
$i_{\text{O}-\text{N}(1)}(\%)$	-0.20	-0.30	-0.20
$i_{\text{N}(1)-\text{C}(1)}(\%)$	-0.30	-0.20	-0.30
$i_{\text{N}(1)-\text{C}(2)}(\%)$	-0.10	-0.20	-0.20
$i_{\text{N}(2)-\text{C}(1)}(\%)$	-1.80	-2.10	-1.90
$i_{\text{N}(2)-\text{C}(3)}(\%)$	-0.80	-0.90	-0.90

Table 10. Structural, magnetic-resonance, electrostatic, and energy parameters of the SC formed by radicals 3–5 with the "frozen" cluster LAS, $\text{Al}(\text{OH})_3$, (coordination through the N atom)

Parameter	3	4	5
$r(\text{Al}\cdots\text{N}(2))/\text{\AA}$	1.97	1.97	1.98
$r(\text{O}-\text{N}(1))/\text{\AA}$	1.22	1.22	1.22
$r(\text{N}(1)-\text{C}(1))/\text{\AA}$	1.53	1.53	1.53
$r(\text{N}(1)-\text{C}(2))/\text{\AA}$	1.51	1.52	1.52
$r(\text{N}(2)-\text{C}(1))/\text{\AA}$	1.50	1.50	1.50
$r(\text{N}(2)-\text{C}(3))/\text{\AA}$	1.32	1.32	1.32
$a^{\text{N}(1)}_{\text{iso}}/\text{Oe}$	19.00	19.00	19.00
$\rho^{\text{N}(1)}$	0.37	0.39	0.38
ρ^{O}	0.61	0.61	0.61
Q^{Al}	0.87	0.87	0.87
$Q^{\text{N}(1)}$	-0.13	-0.13	-0.12
$Q^{\text{N}(2)}$	-0.24	-0.24	-0.24
Q^{O}	-0.22	-0.22	-0.23
Q^{R}	0.29	0.29	0.29
$ \mu /\text{D}$	5.70	5.60	5.70
$\Delta E_c/\text{kcal mol}^{-1}$	-32.20	-29.20	-29.40
$i_{\text{O}-\text{N}(1)}(\%)$	-0.20	-0.30	-0.20
$i_{\text{N}(1)-\text{C}(1)}(\%)$	-0.30	-0.30	-0.30
$i_{\text{N}(1)-\text{C}(2)}(\%)$	-0.10	-0.20	-0.20
$i_{\text{N}(2)-\text{C}(1)}(\%)$	-2.30	-2.70	-2.70
$i_{\text{N}(2)-\text{C}(3)}(\%)$	-1.60	-1.60	-1.40

radicals 2–5 to the model cluster LAS, $\text{Al}(\text{OH})_3$. Taking into account the experimental data described above, we shall analyze two structural types of clusters (see Scheme 4) reflecting the possibility of coordination through both the O and N atoms. By analogy with the paramagnetic SC formed by tanane, we consider the coordination structures in which the geometry of the model cluster LAS has been either fully optimized or "frozen."

The results of calculations carried out for the paramagnetic SC with full optimization of the geometry and assuming coordination at the O atom (see Scheme 4, *a*, *b*) are presented in Table 7. It should be noted that the geometric parameters characterizing individual radicals 2–5 (see Table 6) have barely changed. Most of all, this is true for the lengths of the $\text{N}(2)-\text{C}(1)$ and $\text{N}(2)-\text{C}(3)$ bonds that are remote from the site of coordination. The $r(\text{O}-\text{N})$ distance also hardly changes upon coordination, although the $r(\text{N}(1)-\text{C}(1))$ and $r(\text{N}(1)-\text{C}(2))$ distances are somewhat longer than those in the individual radicals. The ϕ angle, as in the previous cases, does not deviate markedly from 15° , i.e., it is only slightly sensitive to coordination.

The constants of isotropic HFC with ^{27}Al (see Table 7) calculated for all of the SC under consideration are still appreciably underestimated, while those with ^{14}N are close to experimental values and are larger in magnitude than the corresponding values for isolated radicals; this reflects the displacement of the spin density to the N atom upon coordination, which can be

detected by ESR. As in tanane, in radicals 2–5, this displacement results in an inverted ratio of the total spin populations ρ^{N} and ρ^{O} of the N and O atoms. Apparently, this inversion is typical of any nitroxide coordinated through the O atom. Also characteristic is the fact that the charge on the O atom virtually does not change upon coordination, while that on the N(1) atom markedly decreases and approaches zero (see Table 6 and 7).

It is of interest to compare the results of similar calculations of coordinated radicals 2–5 (see Table 7) with those of SC I formed by tanane (see Table 5). As should be expected, the optimized structural characteristics of the model LAS such as the length of the intra-cluster Al–O bond and the α angle do not depend on the structure of the adsorbed radicals, i.e., in all of the cases, this bond is still markedly shorter than the $r(\text{Al}-\text{O})$ distance in alumina found experimentally, and the LAS itself is substantially flattened. Radicals 2–5, which contain 5-membered rings, are prone to form less linear coordinated structures than tanane as indicated by larger θ angles.

The somewhat increased constants of isotropic HFC with the $^{14}\text{N}(1)$ nucleus in the series of both nitroxides 1–5 themselves (see Scheme 2) and the structures formed upon their coordination through the O atom (see Scheme 4, *a*, *b*) are generally consistent with the results obtained for tanane and agree qualitatively with experimental results.^{3,24} It is of interest that the total spin population ρ^{N} of the N(1) atom in tanane is somewhat lower than those in individual imidazolidine and imidazoline radicals (see Tables 5 and 6). At the same time, the spin population of the N(1) atom in the paramagnetic SC I derived from tanane (see Table 5) is markedly higher than those in all analogous cluster structures (see Table 7). This implies that the extent of displacement of the spin density to the N(1) atom following the coordination of tanane is much greater than that in the case of imidazolidine and imidazoline nitroxides.

Unlike spin characteristics, the charge on the Al atom depends little on the type of the coordinated nitroxide. Despite the substantial differences between the charges on the O and N(1) atoms in the cluster SC I of tanane (see Table 5) and in the similar SC of radicals 2–5 (see Table 7), caused by coordination, the extent of the transfer of the electron density Q^{R} from any radical to the model LAS remains virtually constant and reflects the similarity in the formation of complexes by all these paramagnetic compounds. Like individual nitroxides 2–5, their SC under consideration possess smaller dipole moments than the SC I of tanane; besides, the dipole moments of imidazoline cluster structures are smaller than those of the imidazolidine clusters. However, in view of the identical extents of the electron transfer in all the SC under study, the differences between the dipole moments should apparently be explained by the specific structures of the radical fragments in these SC rather than by substantial differences

in the character of coordination of various nitroxides to the model cluster LAS, $\text{Al}(\text{OH})_3$.

Like the positive charges Q^R of the radical fragments in the paramagnetic SC with fully optimized geometries (see Table 7), the calculated energies ΔE_c of the coordination of radicals 2–5 to the LAS through the O atom (see Scheme 4, *a*, *b*) are close to the corresponding value found for SC 1 formed by tanane (see Table 5). As noted above, this value deviates markedly from the experimental values of energies of the formation of donor-acceptor complexes of nitroxides with the surface LAS of alumina. It can be seen from the indices i_{AB} characterizing the change in the strengths of the A–B chemical bonds and listed in Table 7 that coordination has no effect on the N(2)–C(1) and N(2)–C(3) bonds, whereas the N(1)–C(1) and N(1)–C(3) bonds are markedly weakened upon coordination and the N–O bond becomes somewhat stronger.

Table 8 presents the characteristics of structurally similar SC with the "frozen" cluster LAS, $\text{Al}(\text{OH})_3$. In these SC, the donor-acceptor Al...O bond is considerably shorter (*cf.* $r(\text{Al}...\text{O})$ in Tables 7 and 8), and its length is now close to that determined experimentally for alumina.¹⁷ Evidently, this is due to the fixation of the α angle, which imposes the shape of a regular truncated tetrahedron on the model LAS. "Freezing" of the $\text{Al}(\text{OH})_3$ cluster changes the structural parameters of the coordinated nitroxides; in particular, the factor of nonlinearity of the Al–O–N fragment (the θ angle) increases and the extent of pyramidity of the N atom (the φ angle) decreases. At the same time, the length of the distant N(2)–C(3) bond remains unchanged.

From comparison of the data presented in Tables 7 and 8, it can be seen that the constant of isotropic HFC with the ^{14}N nucleus is little sensitive to structural changes in the cluster LAS and in the coordinated radical, whereas the $\rho^{\text{N}} : \rho^{\text{O}}$ ratio markedly increases and becomes practically identical with that found for the paramagnetic SC of tanane (see Table 5). The charges on the Al and N(1) atoms substantially decrease in magnitude as a result of the fixation of the structure of the model LAS, while the charges on the O and N(2) atoms were almost unchanged. The extent of the electron transfer from the coordinated radical to the cluster appreciably increases, which means that they are bound more efficiently to each other. The fact that the dipole moments become markedly greater also attests to significant electronic and structural rearrangements.

In the case of the "frozen" cluster LAS, the energies ΔE_c of complex formation are all close to 30 kcal mol^{–1} (see Table 8), which is in relatively good agreement with the values found experimentally for the chemisorption of some nitroxides on oxide catalysts.² Although the ΔE_c values listed in Table 8 differ appreciably from those presented in Table 7, their behavior is described qualitatively in a similar way. The N–O chemical bond in the paramagnetic SC based on the "frozen" cluster LAS is strengthened to a lesser extent, whereas the N(1)–C(1)

and N(1)–C(2) bonds are weakened even more substantially, which is indicated by the corresponding i_{A-B} indices (see Tables 7 and 8). Thus, as in the case of coordination of H_2NO and tanane, fixation of the geometry of the model LAS makes it possible to achieve better agreement with experimental results, first of all, for the energy of complex formation and the properties directly related to it.

Our quantum-chemical calculations, like radio-spectroscopic studies,^{3,4} made it possible to conclude that no coordination through the N(2) atom occurs in the case of imidazolidine nitroxide 2 (see Scheme 4, *c*). Conversely, imidazoline radicals 3–5 form relatively stable paramagnetic SC with the cluster LAS $\text{Al}(\text{OH})_3$ (see Scheme 4, *d*). The structural, magnetic-resonance, electrostatic, and energy parameters of these SC are listed in Tables 9 and 10.

Comparison of the data listed in Tables 7 and 9 demonstrates that the length of the intra-cluster Al–OH bond in the model LAS and the extent of its pyramidity (the α angle) virtually do not depend on the manner of coordination. Small sensitivities to the type of complex formation are also observed for the lengths of the chemical bonds in nitroxides 3–5. However, in the case of coordination by the O atom (see Table 7), the $r(\text{Al}...\text{N}(2))$ distance (see Table 9) is much longer than $r(\text{Al}...\text{O})$; therefore, the effect of the cluster LAS on the electronic structure and the spin properties of the radical subsystems in the corresponding paramagnetic SC (see Scheme 4, *d*) should be much weaker, which can be judged from the indices characterizing the change in the strengths of the O–N and N–C chemical bonds.

The constants of isotropic HFC with $^{14}\text{N}(1)$ in individual radicals 3–5 (see Table 6) and in the same radicals coordinated at the N(2) atom (see Table 9) are nearly identical. This is not surprising in view of the fact that the nitroxyl group carrying the unpaired electron is far removed from the site of coordination. For the same reason, the ratio of the total spin populations for this SC, $\rho^{\text{O}} : \rho^{\text{N}} \cong 0.6 : 0.4$, is also characteristic of free nitroxides; this is also confirmed by the data of ESR spectroscopy.^{3,4}

When radicals 3–5 are coordinated through the N(2) atom (see Table 9) rather than through the O atom (see Table 7), the positive charges on the Al atoms found for the SC with full optimization of the geometry are noticeably smaller. Somewhat unexpectedly, both N atoms and the O atom in these SC were found to carry nearly the same charges as those in individual radicals 3–5 (see Table 6), although the degree of the transfer of electron density from the radical fragments to the cluster LAS is considerably greater than that in the case of coordination through the O atom. The dipole moments of the three SC under consideration are close to one another but are much smaller than those of the structures coordinated at the O atom (see Table 7). At the same time, the corresponding energies of complex formation ΔE_c depend little on the manner of coordina-

tion of nitroxides 3–5 to the model cluster LAS, $\text{Al}(\text{OH})_3$.

Table 10 presents the parameters of coordination of the radicals found with the assumption that the structure of the surface LAS is "frozen" as a regular truncated tetrahedron. Many characteristics calculated with this assumption (see Table 10) are virtually identical with those presented above (see Table 9); however, some significant distinctions are also manifested. In particular, the $\text{Al}\cdots\text{N}(2)$ coordination bond is much shorter in all cases, the charge on the Al atom is markedly smaller, and the degree of the electron transfer from the coordinated radical to the cluster is substantially greater; therefore, the dipole moment and the energy of complex formation also increase.

It is of special interest to carry out comparative quantum-chemical analysis of the energy characteristics of the coordination of nitroxides 2–5 to the model cluster LAS. As in the case of tanane, energies of complex formation close to those measured experimentally were obtained in the calculations for paramagnetic SC with a fixed geometry of the cluster (see Tables 8 and 10). Therefore, the results of exactly these calculations can be used for the estimation of the predominant ways of coordination of radicals 2–5.

Our calculations, which are in full agreement with the experimental results,^{3,4} have shown that imidazolidine radicals are prone to coordination only through the O atom. The difference ($\sim 3 \text{ kcal mol}^{-1}$) between the energies of formation of the two types of paramagnetic SC (see Scheme 4, *b*, *d*) found by calculations serves as a serious argument for the predominant coordination of radical 3 through the $\text{N}(2)$ atom, because, according to the Boltzmann distribution, the populations of these configuration states can differ by more than two orders of magnitude at the standard temperature. The conclusions drawn from the quantum-chemical analysis for nitroxides 4 and 5 are not so unambiguous, since the calculated energies of their donor-acceptor binding to the model cluster LAS through the nitrogen and oxygen atoms are quite close to each other, which is apparently due to the steric effects arising in the complex formation.

Conclusion

Stable nitroxides often prove to be convenient and highly informative probes in studies of the nature of the surface LAS on Al_2O_3 , since they allow the use of ESR spectroscopy. Owing to the extreme sensitivity of the spin-Hamiltonian parameters to various factors of coordination, the ESR spectra of coordinated nitroxides can be used successfully to solve structural-chemical problems associated with the reliable identification of the donor-acceptor SC, which is needed for advancing a justified concept of the elementary steps of acid-base

processes involving reactive LAS. However, reliable interpretation of radiospectroscopic data relating them to the structural and other physicochemical properties of the resulting paramagnetic SC usually requires that rather complicated quantum-chemical calculations of the magnetic-resonance parameters be carried out by adequate nonempirical or semiempirical methods.¹⁶

The results of the cluster quantum-chemical analysis indicate that the length of the O–N chemical bond, the angle characterizing the pyramidal shape of the N atom, the constants of isotropic HFC with ^{14}N , and the total spin populations of the nitrogen ρ^{N} and oxygen ρ^{O} atoms estimated using the UHF/3-21G and UHF/6-31G nonempirical approaches are in better agreement with the regularities established experimentally than those estimated in terms of similar STO-3G and STO-6G versions. However, semiempirical approaches such as MNDO reproduce the whole set of structural, radio-spectroscopic, and energy parameters characterizing the coordination of nitroxides even more adequately than the nonempirical methods mentioned. Together with the fact that the MNDO approach requires much less computer time, this is the basis to prefer the MNDO method for the cluster quantum-chemical analysis of the physicochemical properties of paramagnetic SC formed by the surface LAS of alumina and complex nitroxide probes.

In the simulation of the chemisorption of nitroxides on the surface of Al_2O_3 , it is more reasonable to fix rigidly the structure of cluster LAS based, for example, on crystallographic data than to determine the structure using a calculation procedure of energy optimization, because the former approach makes it possible to achieve better agreement with the energies of complex formation found experimentally. In addition, when this approach is used, the inversion of the ratio of the total spin populations ρ^{N} and ρ^{O} occurring upon coordination through the O atom that is detected by ESR in all of the nitroxide probes tested is reproduced automatically.

Within the framework of the cluster approach under consideration, some specific features observed in the ESR spectra of imidazolidine and imidazoline nitroxides, which contain two electron-donating sites, bound to Al_2O_3 can be interpreted quantum-chemically. A non-contradictory explanation of these peculiar features is that, owing to energy factors for example, 2,2,3,4,5,5-hexamethyl-3-imidazolidine *N*-oxyl is coordinated to the surface LAS only through its O atom, whereas 2,2,4,5,5-pentamethyl-3-imidazolidine *N*-oxyl is bound mostly by the N atom; finally, in the case of 2,4,5,5-tetramethyl-2-phenyl-(or 2-octyl)-3-imidazolidine *N*-oxyl, the ESR spectrum reflects competing coordination through the two electron-donating sites.

This work was carried out with the financial support of the Russian Foundation for Basic Research (Project No.95-03-08196a).

References

1. A. L. Buchachenko and A. M. Vasserman, *Stabil'nye radikaly* [*Stable Radicals*], Mir, Moscow, 1973, 408 pp. (in Russian).
2. V. B. Golubev, E. V. Lunina, and A. K. Selivanovskii, *Usp. Khim.*, 1981, **50**, 792 [*Russ. Chem. Rev.*, 1981, **50** (Engl. Transl.)].
3. E. V. Lunina, G. L. Markaryan, O. O. Parenago, and A. V. Fionov, *Coll. Surf.*, 1993, **72**, 333.
4. E. V. Lunina, in *Kataliz* [*Catalysis*], Izd. MGU, Moscow, 1987, 287 (in Russian).
5. E. V. Lunina, *App. Spectr.*, 1996, **50**, 1413.
6. E. G. Rozantsev and V. D. Sholle, *Organicheskaya khimiya svobodnykh radikalov* [*Organic Chemistry of Free Radicals*], Khimiya, Moscow, 1979, 344 pp. (in Russian).
7. A. V. Fionov, E. V. Lunina, and N. D. Chuvylkin, *Zh. Fiz. Khim.*, 1993, **67**, 485 [*J. Phys. Chem. USSR*, 1993, **67** (Engl. Transl.)].
8. N. D. Chuvylkin and V. A. Korsunov, *Zh. Fiz. Khim.*, 1983, **57** [*J. Phys. Chem. USSR*, 1983, **57** (Engl. Transl.)].
9. N. D. Chuvylkin and V. B. Kazanskii, *Zh. Fiz. Khim.*, 1987, **61**, 756 [*J. Phys. Chem. USSR*, 1987, **61** (Engl. Transl.)].
10. N. D. Chuvylkin and G. M. Zhidomirov, *Zh. Fiz. Khim.*, 1981, **55**, 1 [*J. Phys. Chem. USSR*, 1981, **55** (Engl. Transl.)].
11. N. D. Chuvylkin, *Zh. Fiz. Khim.*, 1985, **59**, 1085 [*J. Phys. Chem. USSR*, 1985, **59** (Engl. Transl.)].
12. G. M. Zhidomirov and N. D. Chuvylkin, *Usp. Khim.*, 1986, **55**, 353 [*Russ. Chem. Rev.*, 1986, **55** (Engl. Transl.)].
13. I. N. Senchenya, N. D. Chuvylkin, and V. B. Kazanskii, *Kinet. Katal.*, 1986, **27**, 608 [*Kinet. Catal.*, 1986, **27** (Engl. Transl.)].
14. V. M. Gun'ko, D. Sc. (Chem.) Thesis, IKhP NANU, Kiev, 1995 (in Russian).
15. *A Handbook of Computational Chemistry*, Wiley, New York, 1985.
16. G. M. Zhidomirov, P. V. Schastnev, and N. D. Chuvylkin, *Kvantovo-khimicheskie raschety magnitno-rezonansnykh parametrov* [*Quantum-Chemical Calculations of Magnetic-Resonance Parameters*], Nauka, Novosibirsk, 1978, 368 pp. (in Russian).
17. A. J. Leonard, P. N. Semaille, and J. J. Fripiat, *Proc. Brit. Ceram. Soc.*, 1969, 103.
18. P. Bischof and G. Friedrich, *J. Comp. Chem.*, 1982, **3**, 486.
19. N. D. Chuvylkin, I. Yu. Shchapin, V. L. Klochikhin, V. A. Tikhomirov, and V. I. Fel'dman, *Vestn. Mosk. Un-ta* [*Bull. Moscow Univ.*], 1992, **33**, 307 (in Russian).
20. I. Yu. Shchapin, V. I. Fel'dman, V. N. Belevskii, N. A. Donskaya, and N. D. Chuvylkin, *Izv. Akad. Nauk, Ser. Khim.*, 1995, 212 [*Russ. Chem. Bull.*, 1995, **44**, 203 (Engl. Transl.)].
21. I. Yu. Shchapin and N. D. Chuvylkin, *Izv. Akad. Nauk, Ser. Khim.*, 1996, 321 [*Russ. Chem. Bull.*, 1996, **44**, 306 (Engl. Transl.)].
22. N. D. Chuvylkin and G. M. Zhidomirov, *Kvantovaya khimiya i organicheskii kataliz. Ser. kinetika i kataliz* [*Quantum Chemistry and Organic Catalysis. Ser. Kinetics and Catalysis*], VINITI, Moscow, 1980, **8** (in Russian).
23. G. M. Zhidomirov and I. D. Mikheikin, *Klasternoe priblizhenie v kvantovo-khimicheskikh issledovaniyakh khemosorbtsii i poverkhnostnykh struktur. Ser. Siroenie molekul i khimicheskaya svyaz'* [*Cluster Approximation in Quantum-Chemical Studies of Chemisorption and Superficial Structures. Ser. Molecular Structure and Chemical Bond*], VINITI, Moscow, 1984, **9** (in Russian).
24. L. B. Volodarskii, I. A. Grigor'ev, S. A. Dikanov, V. A. Reznikov, and G. I. Shchukin, *Imidazolinovye nitroksil'nye radikaly* [*Imidazoline Nitroxides*], Nauka, Sib. Otd., Novosibirsk, 1988, 216 pp. (in Russian).

Received March 18, 1997